

# Origin of the High Electrical Conductivity of Neutral [Ni(ptdt)<sub>2</sub>] (ptdt<sup>2-</sup> = propylenedithiotetrathiafulvalenedithiolate): A Route to Neutral Molecular Metal

Akiko Kobayashi,<sup>\*,†</sup> Hisashi Tanaka,<sup>†</sup> Mieko Kumasaki,<sup>†</sup> Hajime Torii,<sup>†</sup> Bakhyt Narymbetov,<sup>‡</sup> and Takahumi Adachi<sup>‡</sup>

Contribution from the Research Centre for Spectrochemistry, Graduate School of Science, The University of Tokyo, Hongo, Bunkyo-ku, Tokyo 113-0033, Japan, and the Institute for Molecular Science, Myo-daiji Chyo, Okazaki, Aichi 444-8585, Japan

Received June 21, 1999

**Abstract:** A novel neutral nickel complex molecule with the extended TTF dithiolato ligand, propylenedithiotetrathiafulvalenedithiolate [ptdt<sup>2-</sup> = (S<sub>8</sub>C<sub>9</sub>H<sub>6</sub>)<sup>2-</sup>], was synthesized. In the [Ni(ptdt)<sub>2</sub>] crystal, [Ni(ptdt)<sub>2</sub>] molecules form one-dimensional columns along the *a* axis, having short intermolecular transverse S...S contacts. The crystal exhibited an extremely high electrical conductivity (7 S cm<sup>-1</sup>) at room temperature as a neutral molecular crystal. High-pressure resistivity measurements were made up to 72 kbar, which revealed that the resistivity could not be suppressed by applying high pressure unlike the usual highly conducting low-dimensional organic conductors. The tight-binding band structure calculation indicated that the HOMO (highest occupied molecular orbital) and the LUMO (lowest unoccupied molecular orbital) formed "crossing bands", whose Fermi surfaces tended to vanish due to the HOMO-LUMO interactions. Only very small electron and hole pockets appeared in the Fermi surface due to the transverse interactions between neighboring columns. On the basis of these analyses, the requirements for the development of molecular metals composed of single molecules are discussed.

## Introduction

There seems to be an increasing interest in developing highly conducting or metallic systems based on transition metal complex molecules with extended-TTF-like dithiolato ligands.<sup>1-6</sup> From the viewpoint of molecular design, there are presently some important targets for the chemistry of molecular conductors. The design of a metal composed of single-component neutral molecules is one of the targets of the molecular design. We have recently found that crystals based on [Ni(ptdt)<sub>2</sub>] molecules (ptdt<sup>2-</sup> = propylenedithiotetrathiafulvalenedithiolate) had the room temperature conductivity of about 7 S cm<sup>-1</sup>, which was almost comparable with that of molecular metals based on other multi-sulfur  $\pi$  molecules such as BEDT-TTF (bis(ethylenedithio)tetrathiafulvalene)<sup>7</sup> and M(dmit)<sub>2</sub> (M = Ni, Pd; dmit = 4,5-dimercapto-1,3-dithiole-2-thione).<sup>8</sup>

The two main requirements in the design of molecular metals are (1) the formation of an electronic band and (2) the generation of charge carriers. That is, the establishment of a metallic state

in the molecular system requires (a) effective intermolecular overlap of frontier orbitals to form a delocalized electronic band and (b) partial occupation by electrons of the delocalized energy band.

A transition-metal complex, such as the [M(dmit)<sub>2</sub>] species, can exist as the dianion, the monoanion, or the neutral complex.<sup>8</sup> In the dianion complex, the LUMO will contain a pair of electrons and, therefore, any delocalized band formed by intermolecular overlap of the LUMOs will be completely filled, resulting in semiconducting properties. Similarly, the neutral complex with a completely filled HOMO band will be semiconducting, while the monoanion will contain a single electron in the LUMO and, therefore, in this case, the resulting delocalized band would be expected to be half-filled. It is well-known that such a system would be very susceptible to the Peierls instability<sup>9</sup> resulting in the formation of a dimeric structure or the electron localization effect due to electron correlation.<sup>10</sup> Consequently, the system tends to be insulating. Also, the partial occupation of the conduction band seems to be inevitable for the formation of free carriers. This has only been realized and reported by the charge transfer between two

<sup>†</sup> The University of Tokyo.

<sup>‡</sup> Institute for Molecular Science.

(1) Narvor, N. L.; Robertson, N.; Weyland, T.; Killburn, J. D.; Underhill, A. E.; Webster, M.; Svenstrup, N.; Becker, J. *J. Chem. Soc., Chem. Commun.* **1996**, 1363–1364.

(2) Narvor, N. L.; Robertson, N.; Wallace, E.; Killburn, J. D.; Underhill, A. E.; Bartlett, P. N.; Webster, M. *J. Chem. Soc., Dalton. Trans.* **1996**, 823–828.

(3) Kumasaki, M.; Tanaka, H.; Kobayashi, A. *J. Mater. Chem.* **1998**, *8*, 301–307.

(4) Kobayashi, A.; Kumasaki, M.; Tanaka, H. *Synth. Met.* **1999**, 1768–1769.

(5) Nakano, M.; Kuroda, A.; Maikawa, T.; Matsubayashi, G. *Mol. Cryst. Liq. Cryst.* **1996**, *284*, 301–305.

(6) Ueda, K.; Goto, M.; Iwamatsu, M.; Sugimoto, T.; Endo, S.; Toyota, N.; Yamamoto, K.; Fujita, H. *J. Mater. Chem.* **1998**, *8*, 2195–2198.

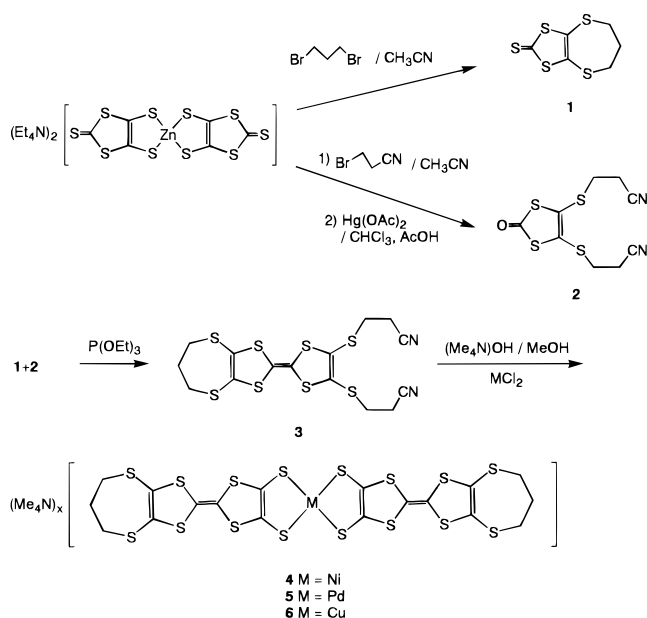
(7) Williams, J. M.; Ferraro, J. R.; Thorn, R. J.; Carlson, K. D.; Geiser, U.; Wang, H. H.; Kini, A. M.; Whangbo, M.-H. *Organic Superconductors*; Prentice Hall: Englewood Cliffs, NJ, 1992).

(8) Kobayashi, A.; Kobayashi H. Molecular Metals and Superconductors Based on Transition Metal Complexes. In *Handbook of Organic Conductive Molecules and Polymers*; Nalwa, H. S., Ed.; John Wiley & Sons, Ltd.: New York, 1997; Vol. I, pp 249–291.

(9) Kagoshima, S.; Nagasawa H.; Sambongi T. *One-Dimensional Conductors*; Springer Series in Solid-State Sciences No. 72; Springer-Verlag: Berlin, Heidelberg, 1988.

(10) Yoneyama, N.; Miyazaki A.; Enoki T.; Saito G. *Bull. Chem. Soc. Jpn.* **1999**, 639–651.

## Scheme 1



- 1: 4,5-propylenedithio-1,3-dithiole-2-thione  
 2: 4,5-bis(2-cyanoethylthio)-1,3-dithiole-2-one  
 3: 2,3-bis(2-cyanoethylthio)-6,7-propylenedithiotetrathiafulvalene

(or more) species constructing the molecular conductors. Thus the development of metallic compound based on a single neutral molecule is a very challenging problem.

In this paper we will demonstrate high conductivity in neutral nickel dithiolene complexes achieved by using an extended ligand with a TTF skeleton. The reason this compound has such a high electrical conductivity will be clarified by the crystal structure determination, the electronic structure calculations, and the high-pressure resistivity measurements. A possible way to realize a neutral metallic compound composed of a single component molecule will be discussed based on the consideration of the band structure of  $[\text{Ni}(\text{ptdt})_2]$ .

## Experimental Section

**Synthesis and Crystal Growth.** The tetrathiafulvalenedithiolates were prepared following the method of Narvor et al.<sup>1,3</sup> The  $\text{ptdt}^{2-}$  (propylenedithiotetrathiafulvalenedithiolate) ligand was synthesized as shown in Scheme 1.

Gemmell et al.<sup>11</sup> and Misaki<sup>12</sup> reported that their unsymmetrical TTF derivatives were obtained in high yields using *p*-acetoxybenzyl. We first used *p*-acetoxybenzyl as the protecting group in cross-coupling to synthesize the unsymmetrical precursor of  $\text{ptdt}^{2-}$ . However, the cross-coupling method gave more than five products and our target molecule was obtained in only 4.6% yield. The cyanoethyl was then used as the protecting group, which gave the precursor of  $\text{ptdt}^{2-}$  (3) in high yield (61%). The tetramethylammonium salts of the metal complexes (4, 5, 6) were obtained by deprotection of the cyanoethyl group with  $\text{Me}_4\text{NOH}$  followed by the addition of the methanol solutions of  $\text{MCl}_2$  ( $\text{M} = \text{Ni}, \text{Cu}, \text{and Pd}$ ) at  $-78^\circ\text{C}$ . For the purpose of obtaining the partially oxidized salts of  $[\text{Ni}(\text{ptdt})_2]$ , the electrochemical oxidation was performed.  $\text{Me}_4\text{N}[\text{Ni}(\text{ptdt})_2]$  (12 mg) and barium trithiocarbonate (47 mg) were placed by the addition of acetonitrile and  $\text{Et}_2\text{O}$  (20%) as the solvent in separate compartments of a glass H-cell. The black plate single crystals of the neutral nickel complex were unexpectedly obtained in this procedure of the electrocrystallization using a current of  $0.1 \mu\text{A}$  in an H-shaped cell with platinum electrodes under an argon

atmosphere. The EPMA (electron probe microanalysis) was measured for neutral  $[\text{Ni}(\text{ptdt})_2]$ . The ratio of Ni and S was 1:14.6. No trace of other extra elements was detected.

**Crystal Structure Determination.** Intensity data were collected at room temperature using a Rigaku AFC7R automatic four-circle diffractometer equipped with a rotating anode. However, the quality of the data was not satisfactory because of the twinning of the crystals. To find a crystal available for the structure determination, the crystals were examined using the Weissberg type IP (imaging plate) system (DIP 320S, MAC Science Co., Inc.).<sup>13</sup> The intensity data were successfully collected at room temperature by the Weissberg-type IP system. The monochromatized  $\text{Mo K}\alpha$  radiation ( $\lambda = 0.7107 \text{ \AA}$ ) was used in all X-ray experiments. The crystal data and experimental details at room temperature are listed in Table 1. At room temperature, 2580 intensity data were collected. The crystal structure was determined using 1968 observed reflections larger than  $3\sigma(I)$ . The final  $R$  and  $R_w$  were 0.087 and 0.15, respectively. The weighting scheme was  $\sigma^2(F_o)^{-1}$ . Anisotropic temperature factors were adopted for all the non-hydrogen atoms. The calculated positions of hydrogen atoms [ $d(\text{C}-\text{H}) = 0.95 \text{ \AA}$ ] were included in the final calculation. Atomic scattering factors were taken from the *International Tables for X-ray Crystallography*.<sup>14</sup> All the calculations were performed using the teXsan crystallographic software package from the Molecular Structure Corporation.<sup>15</sup>

The crystal structure determination at 90 and 30 K was performed using the Weissberg-type low-temperature IP (imaging plate) system (DIP 320S, MAC Science Co., Inc.) equipped with a helium refrigerator.<sup>13</sup> The crystal data and experimental details at 90 and 30 K are listed in Table 1. The X-ray structural analysis of  $[\text{Ni}(\text{ptdt})_2]$  at 90 K was satisfactorily completed. All the non-hydrogen atoms were anisotropically refined. The  $R$  value is 0.090 for 1887 ( $I > 3\sigma(I)$ ) independent reflections at 90 K. The structure at 90 K was almost the same as that at room temperature. However, the analysis at 30 K has not been made because of the weakness of the intensities for the observed extra reflections indicating the development of a "superlattice".

**Electrical Resistivity.** Resistivities were measured by the conventional four-probe method using gold wire ( $0.015 \mu\text{m}$ ) with gold paint as the contact in the temperature range of 4–353 K along the direction approximately parallel to the  $a$  axis. High-pressure resistivity measurements were made up to 12 kbar using the usual clamp-type cell, where silicone oil (Idemitsu Daphne No. 7373) was used as the pressure medium. For the much higher pressure, resistivity measurements were made using the diamond anvil cell. There is no established diamond-anvil technique for the four-probe resistivity measurement but we have recently succeeded in obtaining sufficiently accurate single-crystal resistivity data up to 100 kbar by modifying the two-probe method developed by Matsuzaki.<sup>16</sup> Four gold wires ( $5 \mu\text{m}$  phi) were bonded by gold paint to the single crystal of  $[\text{Ni}(\text{ptdt})_2]$  ( $0.28 \times 0.10 \times 0.04 \text{ mm}^3$ ) and put in the four ditches in the stainless steel gasket filled with alumina powder and epoxy resin to maintain the insulation between the gold wires and the gasket. The pressure was monitored by ruby fluorescence. The resistivities of  $[\text{Ni}(\text{ptdt})_2]$  were measured up to 72 kbar and down to 4 K. The success of the four-probe high-pressure resistivity measurements using the diamond-anvil cell will be very useful for future studies on the solid-state properties at high pressure. The details of the four-probe resistivity measurement technique using the diamond-anvil cell will be reported elsewhere.<sup>17</sup>

**Electronic Structure Calculation.** All *ab initio* molecular orbital (MO) and density functional (DF) calculations were performed using Gaussian 94<sup>18</sup> on a Hewlett-Packard workstation (Apollo 9000 series model 735) at the Research Centre for Spectrochemistry of the University of Tokyo, Hitachi SR2201 at the Computer Centre of the University of Tokyo, and IBM SP2 computers at the Computer Center of the Institute for Molecular Science, Okazaki.

(13) Kobayashi, A.; Naito, T.; Kobayashi, H. *Phys. Rev.* **1995**, *B51*, 3198–3201.

(14) *International Tables for X-ray Crystallography*; Kynoch Press: Birmingham, 1974; Vol. IV.

(15) teXsan: Crystal Structure Analysis Package, Molecular Structure Corporation, 1985 and 1992.

(16) Matsuzaki, S. *Synth. Met.* **1993**, *61*, 207–209.

(17) Adachi, T.; Kobayashi, H. To be submitted for publication.

(11) Gemmell, C.; Janairo, G. C.; Kilburn, J. D.; Veck, H.; Underhill, A. *J. Chem. Soc., Perkin Trans.* **1994**, 2715–2720.

(12) Misaki, Y.; Nishikawa, H.; Kawakami, K.; Koyanagi, S.; Yamabe, T.; Shiro, M. *Chem. Lett.* **1992**, 2321–2324.

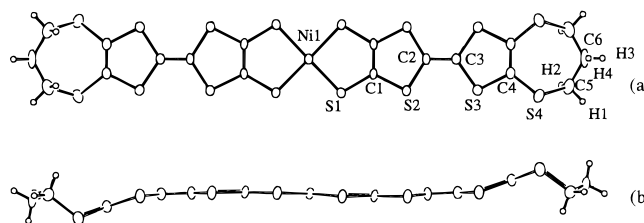
**Table 1.** Crystal Data and Experimental Details for Ni(ptdt)<sub>2</sub> (Chemical Formula NiS<sub>16</sub>C<sub>18</sub>H<sub>12</sub>) at 296, 90, and 30 K

	temperature (K)			
	296	90	30	30 (average)
formula wt	799.95	799.95	799.95	799.95
<i>a</i> /Å	10.096(4)	10.058(6)	10.065(6)	10.067(26)
<i>b</i> /Å	11.802(4)	11.728(6)	11.697(6)	11.666(27)
<i>c</i> /Å	12.42(1)	12.16(1)	46.32(1)	12.14(3)
$\beta$ /deg	108.74(6)	108.11(6)	96.01(5)	108.4(2)
<i>V</i> /Å <sup>3</sup>	1401(1)	1363(1)	5422(4)	1352(1)
space group	<i>C2/m</i>	<i>C2/m</i>	<i>C2/c</i>	<i>C2/m</i>
<i>Z</i>	2	2	8	2
<i>d</i> <sub>v</sub> /g cm <sup>-3</sup>	1.896	1.948	1.960	1.965
dimensions/mm	0.4 × 0.3 × 0.1	0.4 × 0.3 × 0.1	0.4 × 0.3 × 0.1	0.4 × 0.3 × 0.1
radiation	Mo K $\alpha$	Mo K $\alpha$	Mo K $\alpha$	Mo K $\alpha$
data collection	imaging plate	imaging plate	imaging plate	imaging plate
$\mu$ /cm <sup>-1</sup>	18.98	19.50	19.61	19.66
$2\theta_{\max}$ /deg	60.9	61.0	61.0	61.0
total reflcn	2800	2736	10055	2136
reflcn used	2580	2525	9332	1627
$3\sigma(I) < I$	1968	1887	2998	1313
<i>R</i> , <i>R</i> <sub>w</sub>	0.087, 0.150	0.090, 0.167		0.099, 0.125
weighting scheme	1/ $\sigma^2$	1/ $\sigma^2$	1/ $\sigma^2$	1/ $\sigma^2$
GOF	0.14	0.14		4.01

**Table 2.** The Exponents  $\zeta$  and the Ionization Potentials (eV) for Atomic Orbitals

	orbital	$\zeta$	<i>E</i> <sub>i</sub> /eV	orbital	$\zeta$	<i>E</i> <sub>i</sub> /eV	
S	3s	2.122	-20.0	C	2s	1.625	-21.4
	3p	1.825	-11.0		2p	1.625	-11.4
	3d	1.5	-5.44		H	1s	1.0
Ni	4s	2.1	-7.34				
	4p	2.1	-3.74				
	4d	<i>a</i>	-10.6				

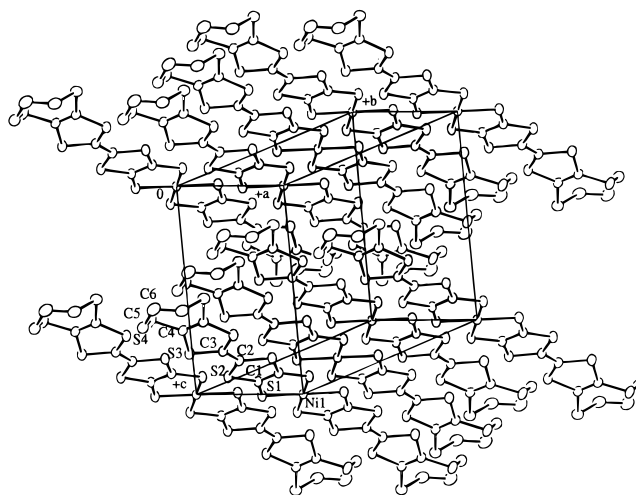
<sup>a</sup> Double  $\zeta$ : 0.5681 $\chi_1$ (5.75) + 0.6294 $\chi_2$ (2.0).

**Figure 1.** (a) An ORTEP drawing of [Ni(ptdt)<sub>2</sub>] at 296 K showing the atom labeling at the 50% probability level. (b) Side view of [Ni(ptdt)<sub>2</sub>].

**Electronic Band Structure Calculation.** The electronic band structures of [Ni(ptdt)<sub>2</sub>] were calculated using the extended Hückel tight-binding approximation on the basis of the highest occupied molecular orbital (HOMO) and the lowest unoccupied molecular orbital (LUMO). The exponents  $\zeta$  and ionization potentials (eV) for the atomic orbitals are listed in Table 2.

## Results and Discussion

**Crystal Structure.** The [Ni(ptdt)<sub>2</sub>] molecule at room temperature is shown in Figure 1 and the selected bond lengths and angles are listed in Table 3. The Ni atoms are located on the *2/m* position, in which the mirror plane includes the long

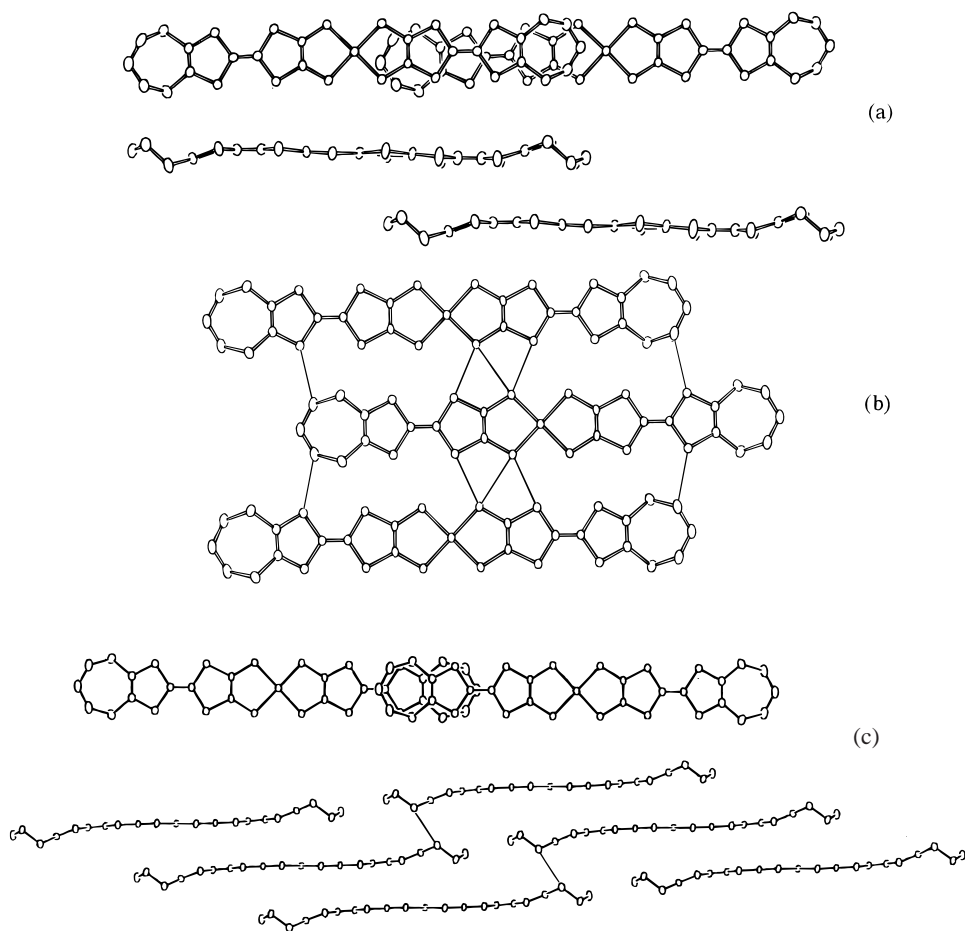
**Figure 2.** The crystal structure of [Ni(ptdt)<sub>2</sub>] at 296 K. [Ni(ptdt)<sub>2</sub>] molecules stack along the [100] directions.

axis of the molecule and is perpendicular to the molecular plane. The geometry around the Ni atom is square-planar and the eight sulfur atoms of the propylenedithio-substituted tetrathiafulvalenyldithiolato ligand are essentially coplanar; however, the terminal propylenic group is bent. The Ni complex shows Ni–S distance of 2.183(1) Å and an S–Ni–S angle of 92.99(5)° (2.186(1) Å, 93.18(7)° at 90 K). The C=C distance in the tetrathiafulvalene ring is 1.380(7) Å (1.373(10) Å at 90 K). The largest deviation from the plane is 1.419 Å (1.483 Å at 90 K). The crystal structure of the neutral [Ni(ptdt)<sub>2</sub>] is shown in Figure 2. The shortest Ni···Ni distance is 7.766(1) Å (7.725(2) Å at 90 K). Similar to the planar  $\pi$  molecules in highly conducting organic crystals, the almost planar [Ni(ptdt)<sub>2</sub>] molecules form a regular column along *a* direction with an interplanar distance of 3.376 Å (3.190 Å at 90 K). The fairly short intermolecular distance (especially at 90 K) indicates the existence of intermolecular interactions. The mode of overlap is shown in Figure 3a. The S atoms in the propylenedithio group overlap on the S atoms bonded to the central Ni atom. The short intermolecular S···S contacts less than the sum of the van der Waals radius at room temperature and at 90 K are shown in Table 4. The shortest S···S intermolecular contact is 3.446(2) Å at room temperature and 3.369(3) Å at 90 K, which is observed along the stacking

(18) Frisch, M. J.; Trucks, G. W.; Schlegel, H. B.; Gill, P. M. W.; Johnson, B. G.; Robb, M. A.; Cheeseman, J. R.; Keith, T.; Petersson, G. A.; Montgomery, J. A.; Raghavachari, K.; Al-Laham, M. A.; Zakrzewski, V. G.; Ortiz, J. V.; Foresman, J. B.; Cioslowski, J.; Stefanov, B. B.; Nanayakkara, A.; Challacombe, M.; Peng, C. Y.; Ayala, P. Y.; Chen, W.; Wong, M. W.; Andres, J. L.; Replogle, E. S.; Gomperts, R.; Martin, R. L.; Fox, D. J.; Binkley, J. S.; Defrees, D. J.; Baker, J.; Stewart, J. J. P.; Head-Gordon, M.; Gonzalez, C.; Pople, J. A.; Gaussian, Inc.: Pittsburgh, PA, 1995.

**Table 3.** Bond Lengths (Å) and Bond Angles (deg) at 296 and 90 K

(a) 296 K					
Ni1–S1	2.183(1)	C1–C1	1.384(8)	S3–C4	1.765(4)
S2–C1	1.736(4)	C4–C4	1.384(8)	S4–C5	1.811(6)
S3–C3	1.752(3)	S1–C1	1.726(4)	C2–C3	1.380(7)
S4–C4	1.743(4)	S2–C2	1.743(3)	C5–C6	1.535(7)
S1–Ni1–S1	92.99(5)	S3–C4–S4	115.8(2)	S1–C1–C1	121.1(1)
Ni1–S1–C1	102.4(1)	S4–C4–C4	127.8(1)	S2–C2–S2	116.1(3)
C3–S3–C4	96.0(2)	C5–C6–C5	118.5(6)	S2–C2–C3	121.9(1)
S1–C1–S2	121.9(2)	S1–Ni1–S1	87.01(5)	S3–C3–C2	123.5(1)
S2–C1–C1	117.0(1)	C1–S2–C2	94.9(2)	S3–C4–C4	116.3(1)
S2–C2–C3	121.9(1)	C4–S4–C5	103.7(2)	S4–C5–C6	115.6(4)
S3–C3–S3	113.1(3)				
(b) 90 K					
Ni1–S1	2.186(1)	C1–C1	1.36(1)	S3–C4	1.756(5)
S2–C1	1.746(5)	C4–C4	1.348(10)	S4–C5	1.811(6)
S3–C3	1.744(4)	S1–C1	1.730(5)	C2–C3	1.373(10)
S4–C4	1.760(5)	S2–C2	1.758(4)	C5–C6	1.537(7)
S1–Ni1–S1	93.18(7)	S3–C4–S4	115.6(3)	S1–C1–C1	121.7(2)
Ni1–S1–C1	101.7(2)	S4–C4–C4	127.6(2)	S2–C2–S2	114.7(4)
C3–S3–C4	95.0(2)	C5–C6–C5	115.7(6)	S2–C2–C3	122.6(2)
S1–C1–S2	121.0(3)	S1–Ni1–S1	86.82(7)	S3–C3–C2	122.9(2)
S2–C1–C1	117.3(2)	C1–S2–C2	95.3(3)	S3–C4–C4	116.7(2)
S2–C2–C3	122.6(2)	C4–S4–C5	103.7(3)	S4–C5–C6	115.6(5)
S3–C3–S3	114.2(4)				

**Figure 3.** (a) The mode of overlaps of  $[\text{Ni}(\text{ptdt})_2]$ . (b) The molecular arrangement of  $[\text{Ni}(\text{ptdt})_2]$  along the transverse direction. (c) The mode of overlaps along the long axis of the molecule.

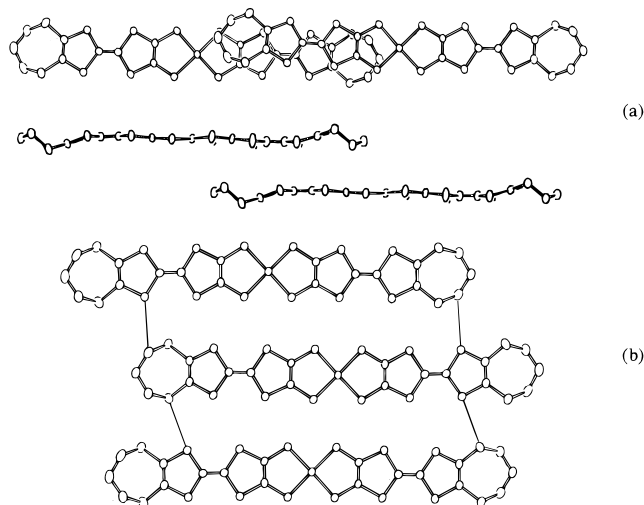
direction. There are short contacts along the transverse direction: 3.526(1), 3.618(2) Å at room temperature and 3.375(2), 3.564(3) Å at 90 K (Figure 3b). In addition to the transverse direction, along the long axis of the molecule, S...S short contacts of 3.499(3) Å at room temperature and 3.418(3) Å at

90 K were observed (Figure 3c). In comparison with the neutral  $[\text{Ni}(\text{ptdt})_2]$  complex, the overlapping mode of the stacking molecules in the 1:1 complex  $(\text{Me}_4\text{N})[\text{Ni}(\text{ptdt})_2] \cdot \text{Me}_2\text{CO}_3^3$  and the molecular arrangements along the transverse direction are shown in Figures 4a and 4b. Comparison of the stacking mode

**Table 4.** Nonbonded Contacts out to 3.70 Å at 296 and 90 K

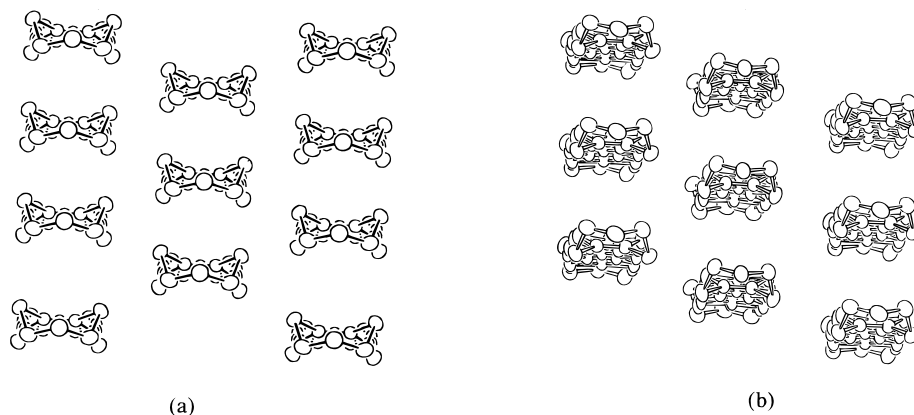
(a) 296 K					
S1–S2	3.526(1) <sup>a</sup>	C1–C3	3.616(7) <sup>e</sup>	S2–S2	3.446(2) <sup>b</sup>
S1–S1	3.618(2) <sup>a</sup>	C6–C6	3.57(1) <sup>f</sup>	S3–C5	3.617(6) <sup>d</sup>
S4–S4	3.499(3) <sup>c</sup>	S1–S3	3.594(2) <sup>b</sup>	C1–C2	3.687(7) <sup>e</sup>
(b) 90 K					
S1–S2	3.475(2) <sup>a</sup>	C1–C2	3.569(8) <sup>e</sup>	S3–C5	3.578(6) <sup>d</sup>
S1–S1	3.564(3) <sup>a</sup>	S1–S3	3.513(2) <sup>b</sup>	C1–C3	3.519(8) <sup>e</sup>
S4–S4	3.418(3) <sup>c</sup>	S2–S2	3.369(3) <sup>b</sup>	C6–C6	3.52(2) <sup>f</sup>
S4–C4	3.618(5) <sup>c</sup>				

<sup>a</sup> Symmetry operation:  $3/2 - X, -1/2 - Y, 2 - Z$ . <sup>b</sup> Symmetry operation:  $1 - X, Y, 2 - Z$ . <sup>c</sup> Symmetry operation:  $-X, Y, 1 - Z$ . <sup>d</sup> Symmetry operation:  $1/2 + X, -1/2 - Y, Z$ . <sup>e</sup> Symmetry operation:  $1 - X, -Y, 2 - Z$ . <sup>f</sup> Symmetry operation:  $-1 - X, -Y, 1 - Z$ .

**Figure 4.** The mode of overlaps of [Ni(ptdt)<sub>2</sub>]<sup>2-</sup> anion in (Me<sub>4</sub>N)[Ni(ptdt)<sub>2</sub>]<sup>2-</sup>·Me<sub>2</sub>CO, (b) the side view of the overlap, and (c) molecular arrangement along the transverse direction.

of the neutral [Ni(ptdt)<sub>2</sub>] and the [Ni(ptdt)<sub>2</sub>]<sup>2-</sup> anion in (Me<sub>4</sub>N)[Ni(ptdt)<sub>2</sub>]<sup>2-</sup>·Me<sub>2</sub>CO<sup>3</sup> is shown in Figures 5a and 5b.

Usually the neutral donor or acceptor molecules have molecular structures and molecular arrangements different from those of the charged molecules incorporated in the complexes. But Figures 3–5 show that the molecular structure and arrangement of the neutral [Ni(ptdt)<sub>2</sub>] fairly resembles those of [Ni(ptdt)<sub>2</sub>]<sup>2-</sup>. Moreover, the molecular arrangement of the neutral [Ni(ptdt)<sub>2</sub>] indicates that the intermolecular overlap along the stacking direction is larger than those in the 1:1 complex. This is very unusual considering that the neutral molecule usually has no attractive interaction between the neighboring molecules except for the weak van der Waals interactions. Thus

**Figure 5.** Comparison of the stacking modes of (a) neutral [Ni(ptdt)<sub>2</sub>] and (b) the [Ni(ptdt)<sub>2</sub>]<sup>2-</sup> anions in (Me<sub>4</sub>N)[Ni(ptdt)<sub>2</sub>]<sup>2-</sup>·Me<sub>2</sub>CO.**Table 5.** Comparison of the Bond Length of Ni–S and the Average C=C Bond Lengths in Ni(ptdt)<sub>2</sub>, [Ni(ptdt)<sub>2</sub>]<sup>2-</sup>, and [Pd(ptdt)<sub>2</sub>]<sup>2-</sup> (1, 2, and 3 Indicate C=C Bond Lengths in ptdt<sup>2-</sup> Shown Below)

	1	2	3	M–S (M = Ni, Pd)
neutral Ni(ptdt) <sub>2</sub> (THF)	1.40	1.38	1.37	2.186(2)
neutral Ni(ptdt) <sub>2</sub> <sup>a</sup>	1.380(7)	1.384(8)	1.357(8)	2.183(1)
Ni(ptdt) <sub>2</sub> <sup>2-</sup> 3	1.342	1.359	1.342	2.168(1)
Pd(ptdt) <sub>2</sub> <sup>2-</sup> 4	1.31	1.34	1.34	2.310(2)

<sup>a</sup> This work.

the short intermolecular contact and large overlap between the neutral [Ni(ptdt)<sub>2</sub>] molecules along the stacking direction and the high conductivity of the neutral crystal will be related to the special electronic structure of the [Ni(ptdt)<sub>2</sub>] crystal.

A comparison of the average C=C bond lengths in [Ni(ptdt)<sub>2</sub>], [Ni(ptdt)<sub>2</sub>]<sup>2-</sup> and [Pd(ptdt)<sub>2</sub>]<sup>2-</sup> is shown in Table 5. It shows that the C=C bond lengths in the [Ni(ptdt)<sub>2</sub>] framework systematically change by varying the formal charge on the molecule.

**Electrical Resistivity.** The electrical conductivities were measured along the *a* axis. The neutral [Ni(ptdt)<sub>2</sub>] is a narrow-gap semiconductor with a room temperature conductivity of 7 S cm<sup>-1</sup>. The electrical resistivity exhibited a monotonic increase down to 60 K with an activation energy of 0.03 eV (Figure 6). Below 60 K, the resistivity increases on lowering the temperature. The single crystal of [Ni(ptdt)<sub>2</sub>] revealed an extremely high electrical conductivity at room temperature as a neutral molecular crystal. It is much higher than the values normally observed for the neutral complexes of the dithiolenes. The crystal of the neutral [Ni(dmit)<sub>2</sub>] is fairly conductive with  $\sigma_{RT} = 3.5 \times 10^{-3}$  S cm<sup>-1</sup>.<sup>19</sup> It is well-known that the resistivity of the neutral molecular crystal is sensitive to the existence of impurities. However, to our knowledge, it seems to be very difficult for the neutral molecular crystal to have a conductivity higher than 10<sup>-2</sup> S cm<sup>-1</sup> even in such cases. If the impurities can produce a conductivity higher than 1 S cm<sup>-1</sup>, many neutral molecular crystals should show such high conductivities. Consequently, it appears unlikely that the high conductivity of the [Ni(ptdt)<sub>2</sub>] crystal, which is almost equal to those of the usual molecular conductors, is due to the impurities. The high conductivities presumably reflect the large intermolecular overlap associated with the use of extended ligand  $\pi$ -systems including a large number of sulfur atoms.

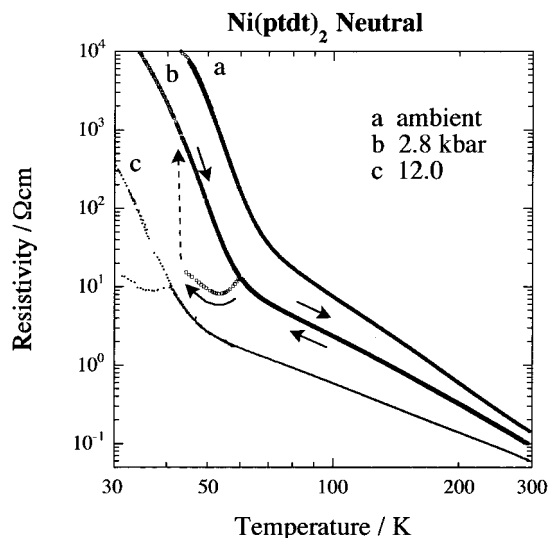


**Figure 6.** The resistivity measurement of [Ni(ptdt)<sub>2</sub>] at ambient pressure and high-pressure resistivity measurement up to 12 kbar using the clamp-type high-pressure cell. The arrows indicate the cooling and heating cycles. The resistivity at 1 bar did not show any hysteresis.

The phase transition from the high-conducting state to the low-conducting state was observed around 60 K at ambient pressure. When the pressure was applied using the usual clamp-type cell, a gradual suppression of the phase transition was observed with increasing pressure. At 12 kbar, the phase transition temperature was observed around 40 K. As shown in Figure 6, the resistivity at 2.8 kbar showed an anomalous minimum for the cooling cycle at about 55 K. At first, this resistivity anomaly was thought to be related to the cracking of the crystal. However, the resistivity measurements at higher pressure showed the systematic pressure dependence of the anomaly, which suggested that this is due to the intrinsic nature of the crystal. The resistivity measurements were performed at 24, 41, and 72 kbar with the four-probe method using the diamond-anvil cell (Figures 7a, 7b, and 7c).<sup>17</sup> The sample was cooled 2 deg per min during both the cooling and heating cycles. The phase transition temperature moved to the lower temperature and took a minimum around 25 kbar (Figure 7d). The room temperature resistivity also exhibited a minimum around 25 kbar (Figure 7e). The high-pressure resistivity measurements at 41 kbar are shown in Figure 7b. During the cooling process, the resistivity was gradually increased down to 44 K, where the resistivity was 4 Ω cm. The resistivity then began to decrease, taking a minimum value of about 0.5 Ω cm. Below 16 K, the resistivity abruptly increased. Thus there was a small “metallic region” within the temperature range of 44–20 K. Above 10 K, the heating process proceeded in almost the same way as in the cooling process. That is, the “metallic” behavior seemed to show almost no hysteresis around 40 kbar. However, the origin of the “metallic region” is not clear. Above ca. 30 kbar, the room temperature resistivity began to increase. Unexpectedly the room temperature resistivity at 72 kbar was a little larger than that at 1 bar. At 72 kbar, the transition below 50 K exhibited a large hysteresis again. Usually it might be expected that the molecular conductor with a fairly high conductivity and small activation energy will be changed to a metallic conductor at high pressure. But the high-pressure resistivity experiments using the [Ni(ptdt)<sub>2</sub>] crystals suggest that the system has a different electronic structure from those of the usual molecular conductors.

**Crystal Structure at 30 K.** The crystal structure studies at 30 K were performed using the Weissenberg-type low-temper-

ature IP system equipped with a helium refrigerator. The resistivity measurements at ambient pressure showed that there is a phase transition from the high-conducting state to the low-conducting state around 60 K. Around 80 K, very faint extra satellite reflections began to be observed. All the reflections collected at 30 K were indexed with the cell parameters  $a = 10.065(6)$  Å,  $b = 11.697(6)$  Å,  $c = 46.32(1)$  Å, and  $\beta = 96.01(5)^\circ$ . This large cell showed the development of a superlattice. The cell parameters of the fundamental cell are  $a = 10.067(26)$  Å,  $b = 11.666(27)$  Å,  $c = 12.14(3)$  Å, and  $\beta = 108.4(2)^\circ$ , which are almost the same as the cell parameters at room temperature. The relation between the large cell and the fundamental cell is shown in Figure 8. The reflection data were collected at 30 K. Although the average crystal structure at 30 K was obtained (Figure 8), the crystal structure determination has not been completed ( $R = 0.23$ ), because the superlattice reflections were very weak and the number of reflections was limited. The structure at 30 K forms a complicated 4-fold structure along the  $c$  axis. The conformation of the terminal propylene groups will be important for the intermolecular interaction along the  $c$  axis. For the clarification of the origin of the superlattice, a detailed analysis of the superstructure will be required. During the heating cycle, the lattice constants at 100 K were determined and the cell parameters were well refined based on the large cell parameters, which indicates that the low-temperature structure derived from the phase transition remains due to the hysteresis.

**Calculation of Ground Electronic State.** To find the origin of the unusually high electrical conductivity of the neutral [Ni(ptdt)<sub>2</sub>] crystal, the electronic structure of [Ni(ptdt)<sub>2</sub>] was calculated by the *ab initio* MO method at the Hartree–Fock (HF) level and by Becke’s three-parameter hybrid DF method<sup>20</sup> using the Lee–Yang–Parr correlation functional<sup>21</sup> (B3LYP). The 3-21G\* and 6-311G\* basis sets installed in the Gaussian 94 program as well as the SVP and TZVP basis sets developed by Ahlrichs and co-workers<sup>22,23</sup> were used. In the SVP basis set, we selected the Ni(3F) basis<sup>22</sup> for the Ni atom. The starting atomic coordinates of [Ni(ptdt)<sub>2</sub>] were used from the crystal structure determination. The end propylenedithio group is fairly distorted from the NiS<sub>4</sub>C<sub>4</sub> plane. However, the optimized molecule has a good planarity and has approximately a  $D_{2h}$  symmetry except for the propylenedithio group. Therefore, the distorted conformation of the end propylenedithio group might be ascribed to the intermolecular interactions. The calculation of the singlet ground state of [Ni(ptdt)<sub>2</sub>] based on the optimized molecular structure at the HF/3-21G\* and HF/6-311G\* levels showed the symmetries  $b_{2g}$  for HOMO and  $b_{1u}$  for LUMO, which are similar to those of the dmit metal complexes. The LUMO with  $b_{2g}$  symmetry has a nodal plane at the central Ni atom but the HOMO has the same symmetry as the HOMO of BEDT-TTF ( $b_{1u}$ ) without the nodal plane on the central C=C bond. The schematic drawings of the HOMO and LUMO orbitals are shown in Figure 9. The calculated energies of the lowest triplet state and the lowest singlet state of [Ni(ptdt)<sub>2</sub>] at the HF/SVP, B3LYP/SVP, and HF/TZVP levels are listed in Table 6. The lowest triplet state was more stable than the lowest singlet state based on the HF/SVP and HF/TZVP level calculations. However, the singlet state was a little more stable than

(19) Cassoux, P.; Valade, L.; Kobayashi, H.; Kobayashi, A.; Clark, R. A.; Underhill, A. E. *Coord. Chem. Rev.* **1991**, *110*, 115–160.

(20) Becke, A. D. *J. Chem. Phys.* **1993**, *98*, 5648–5652.

(21) Lee, C.; Yang, W.; Parr, R. G. *Phys. Rev. B* **1988**, *B37*, 785–789.

(22) Schafer, A.; Horn, H.; Ahlrichs, R. *J. Chem. Phys.* **1992**, *97*, 2571–2577.

(23) Schafer, A.; Huber, C.; Ahlrichs, R. *J. Chem. Phys.* **1994**, *100*, 5829–5835.

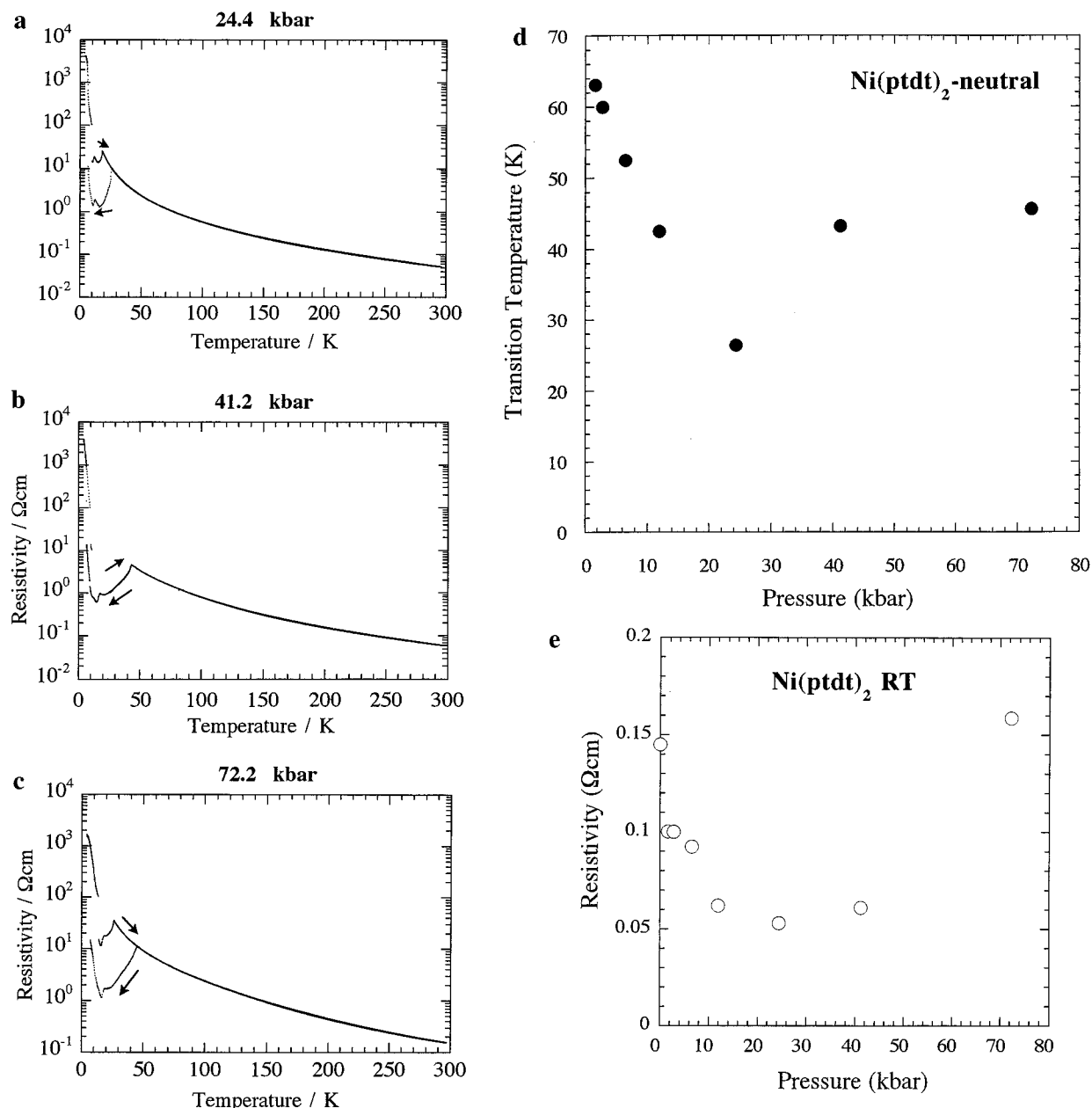


**Figure 7.** High-pressure resistivity measurements with the single-crystal four-probe method using the diamond anvil cell at (a) 24.4, (b) 41.2, and (c) 72.2 kbar. The arrows indicate the cooling or heating process. (d) The pressure dependence of the phase transition temperatures. (e) The pressure dependence of the room temperature resistivity.

the triplet state using the Density Functional Theory (DFT) method B3LYP/SVP. The energy of the lowest triplet electronic state was also calculated at the configuration interaction singles (CIS) level with the SVP basis set. The singlet–triplet energy difference was  $-1.0744$  eV. This result indicated that the lowest triplet state, for which the configuration HOMO  $\rightarrow$  LUMO is predominant, interestingly exists lower than the lowest singlet state.

**Band Structure Calculation.** The high conductivity of the [Ni(ptdt)<sub>2</sub>] crystal presumably reflects the good intermolecular overlap associated with the use of extended  $\pi$ -ligand systems. Simple extended Hückel tight-binding band structure calculations based on HOMO and LUMO were made to obtain a hint for designing the metallic or semimetallic crystals composed of single neutral molecules. According to this approximation,<sup>24</sup> the transfer integral ( $t$ ) was assumed to be proportional to the intermolecular overlap integral of the frontier molecular orbitals of [Ni(ptdt)<sub>2</sub>]. The overlap integrals were calculated based on

the crystal structure at 296 K using Slater-type atomic orbitals, whose semiempirical parameters are listed in Table 2. As previously mentioned, the symmetries of HOMO and LUMO were determined by the *ab initio* calculations of the HF/6-311G\* and HF/3-21G\* levels by Gaussian 94. It was found that the symmetries of the HOMO and LUMO orbitals of [Ni(ptdt)<sub>2</sub>] except for the propylenedithio group are similar to those of [Ni(dmit)<sub>2</sub>]. The HOMO and LUMO obtained using the semiempirical parameters were essentially the same as those determined by the *ab initio* calculations. The overlap integrals are listed in Table 7. The other intermolecular interactions were negligible.

According to the extended Hückel approximation, the energy levels of HOMO and LUMO do not change despite the singlet state or the triplet state. Therefore, both cases have the same HOMO–LUMO energy gap,  $\Delta E$ . As mentioned before, the lowest triplet state seems to be more stable than the lowest singlet state based on the *ab initio* energy calculation. From this result, the HOMO–LUMO energy gap,  $\Delta E$ , in the extended

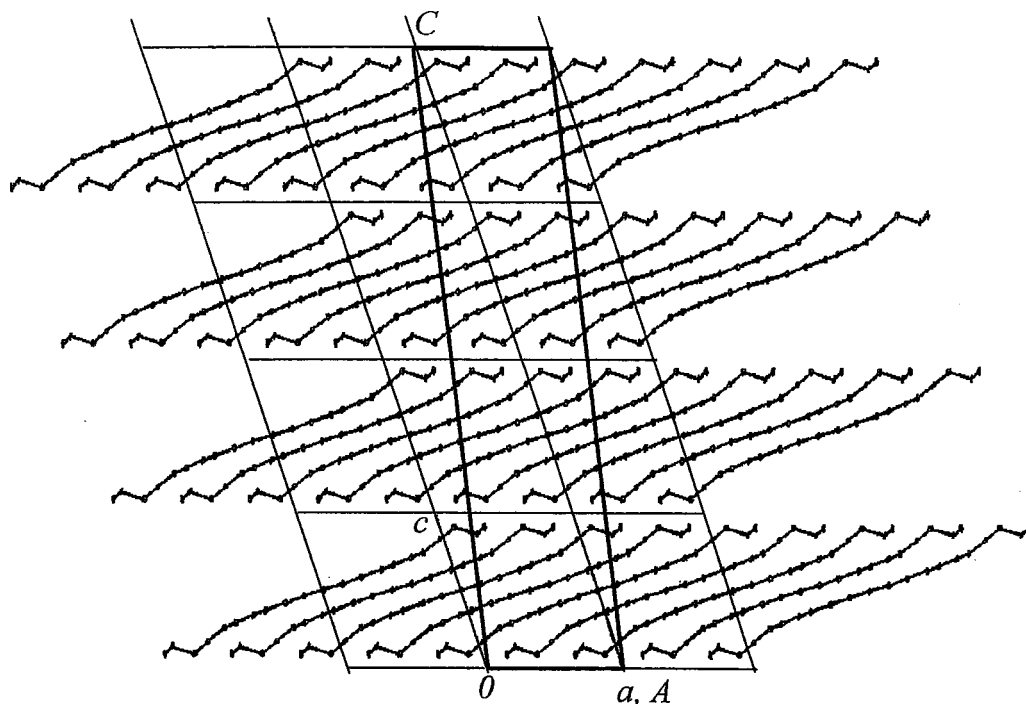


**Figure 8.** The relation between the superlattice and the fundamental cell. A, C and *a*, *c* indicate the superlattice and the fundamental lattice, respectively.

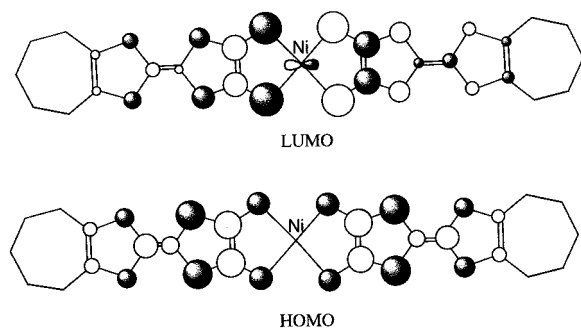


**Figure 9.** The schematic drawings of the HOMO and LUMO orbitals of [Ni(ptdt)<sub>2</sub>].

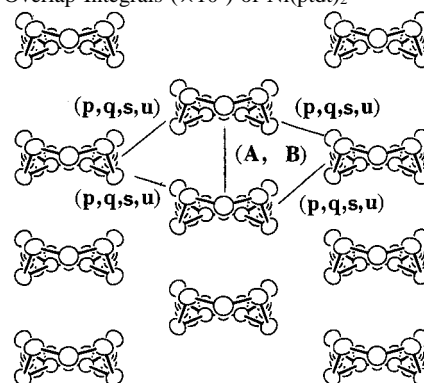
**Table 6.** The Calculated Energies (hartrees) of the Lowest Triplet State and the Lowest Singlet State of [Ni(ptdt)<sub>2</sub>]

	singlet $E(s)$	triplet $E(t)$	$E(t) - E(s)$
HF/SVP	-8552.923622	-8552.975879	-0.052257
B3LYP/SVP	-8570.039066	-8570.031648 (DF)	0.007418
HF/TZVP	-8555.800198	-8555.845342	-0.045144
CIS/SVP		-8552.963106	-0.039484

Hückel calculation can be approximated to be very small. This is consistent with the general tendency that the energy gap between the HOMO and LUMO orbitals becomes smaller as the size of a molecule becomes longer. The band structure calculations were performed by changing  $\Delta E$ . The band structure is dependent only on the ratio of  $\Delta E$  and transfer integral  $t$  ( $=A, B, p, q, \dots$ ). The absolute energy scale is not important in our discussion. Broadly speaking, pressure will increase  $t$ , while  $\Delta E$  is almost independent of pressure. Consequently, we can imagine the band structure at high pressure by reducing  $\Delta E$ .

We have calculated the band structure for various values of  $\Delta E$ . The interstack overlap integrals along the [100] direction are  $14.5 \times 10^{-3}$  for the LUMO-LUMO overlap integral and  $-12.4 \times 10^{-3}$  for the HOMO-HOMO overlap integral. The overlap integral along the transverse direction is about 1/14 as small as that along the chain direction for LUMO-LUMO and

**Table 7.** Overlap Integrals ( $\times 10^3$ ) of Ni(ptdt)<sub>2</sub>



	LUMO-LUMO	HOMO-HOMO	LUMO-HOMO	HOMO-LUMO
<i>A</i>	14.54	<i>B</i> -12.41		
<i>p</i>	-1.02	<i>q</i> -2.12	<i>s</i> -0.26	<i>u</i> 0.26

1/6 that for HOMO-HOMO. Therefore, the electronic band structure of [Ni(ptdt)<sub>2</sub>] is essentially one-dimensional.

The HOMO-LUMO gap of 0.45–0.6 eV is used for the [Ni-(dmit)<sub>2</sub>] compounds.<sup>25</sup> The Fermi surfaces of [Ni(ptdt)<sub>2</sub>] were calculated as a function of  $\Delta E$  ( $=0-0.7$  eV). The Fermi surface has very small electron and hole pockets for a  $\Delta E$  of 0.2, 0.45, and 0.5 eV (Figure 10). The most probable  $\Delta E$  value of [Ni-(ptdt)<sub>2</sub>] will be 0.2–0.45 eV. In the case of  $\Delta E = 0.5$  eV, there remain extremely small electron and hole pockets. When the  $\Delta E$  gap is 0.7 eV, the Fermi surface disappears. The band structure for  $\Delta E = 0.0$  eV will roughly correspond to that at an “extremely high pressure” because the main transfer integrals, *A* and *B*, which are important in determining the energy dispersion curves, are considered to be very enhanced at high

(24) Mori, T.; Kobayashi, A.; Sasaki, Y.; Kobayashi, H. *Chem. Lett.* **1982**, 1923–1926. Mori, T.; Kobayashi, A.; Sasaki, Y.; Kobayashi, H.; Saito, G.; Inokuchi, H. *Bull. Chem. Soc. Jpn.* **1984**, *57*, 627–633.

(25) Kobayashi, A.; Kim, H.; Sasaki, Y.; Kato, R.; Kobayashi, H. *Solid State Commun.* **1987**, *62*, 57–64.



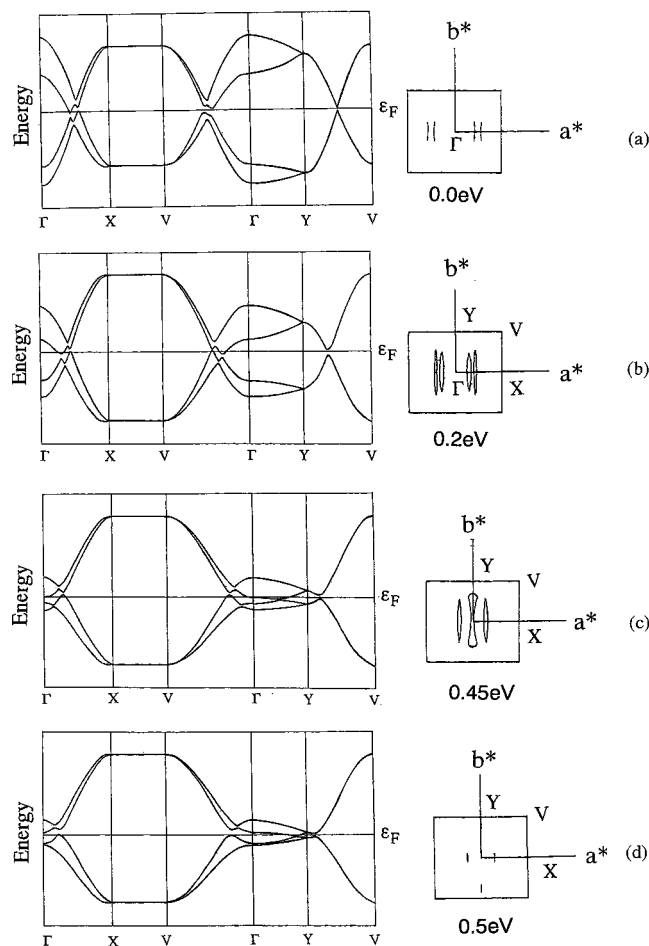


**Figure 10.** The Fermi surfaces and band energies of [Ni(ptdt)<sub>2</sub>] calculated as a function of the HOMO-LUMO gap values (a) 0.0, (b) 0.2, (c) 0.45, and (d) 0.5 eV.

pressure. Unexpectedly, there remains almost no Fermi surface at “high pressure”. The calculations indicate that the [Ni(ptdt)<sub>2</sub>] crystal cannot be metalized by applying pressure (or reducing  $\Delta E$ ) despite the fairly high conductivity at ambient pressure. The enhancement of the resistivity in the higher pressure region (>40 kbar) seems to be consistent with the tendency of the vanishing calculated Fermi surfaces at higher pressure. Thus it may be said that the conductive behavior of this crystal can be qualitatively explained by the simple tight-binding band calculation, despite the fact that the system is not a semimetal but a narrow-gap semiconductor. The most essential point is the “crossing-band formation” of the HOMO and LUMO. Due to the different signs of the overlap integrals of HOMO-HOMO ( $B$ ) and LUMO-LUMO ( $A$ ) (see Table 7) and the relatively small HOMO-LUMO gap, the energy dispersion curves of the HOMO and LUMO bands cross each other at the Fermi level ( $\epsilon_F$ ) but the HOMO-LUMO interaction tends to open a gap at  $\epsilon_F$  resulting in the semiconducting band structure. The very small calculated electron and hole pockets are due to the transverse intermolecular interactions, which would be vanished if slightly larger HOMO-LUMO interactions were used. Although the detailed

structural information on the superlattice could not be obtained, it might be possible to imagine that a small structure modification will produce the very small Fermi surfaces.

## Conclusion

We have prepared the [Ni(ptdt)<sub>2</sub>] crystal, which has a one-dimensional stacking structure of [Ni(ptdt)<sub>2</sub>] molecules. Despite the fairly high conductivity and narrow-gap nature, the resistivity measurements up to 72 kbar have revealed that the crystal cannot be metalized by applying pressure.

On the basis of the band structure examination, the guiding principle of the molecular design of a “neutral metal” composed of a single component molecule can be suggested.

(1) The HOMO-LUMO energy gap must be small. As shown in this study, it will be realized by using the molecules with extended  $\pi$ -ligand frameworks.

(2) The large transverse interactions are desirable, which will permit realizing the semimetallic Fermi surfaces even in the systems with crossing bands.

(3) The molecular arrangement seems to be the most important point to realize a single-component molecular metal. To avoid the formation of the crossing bands, the molecular arrangement, which makes the signs of the overlap integrals of the LUMO-LUMO and HOMO-HOMO interactions the same, must be realized. The HOMO and LUMO then form parallel bands, whose Fermi surfaces are stable against the HOMO-LUMO interaction.

To realize a parallel band, the difference in the symmetries of the HOMO and LUMO orbitals must be considered. The sign of the overlap integral of HOMO-HOMO does not depend on the overlapping mode. On the other hand, the sign of the overlap integral of LUMO-LUMO depends on the overlapping mode due to the fact that the symmetry of the LUMO orbital has a nodal plane at the central Ni atom. Therefore, the sign of the overlap integral of LUMO-LUMO must be minus to form the parallel band. For example, if the slipping direction of two neighboring Ni(ptdt)<sub>2</sub> molecules is along the short axis of the molecules, the parallel bands will be realized as in the case of (DBTTF)[Ni(dmit)<sub>2</sub>].<sup>26</sup>

According to these guiding principles, it might be expected that molecular metals or semimetals composed of single molecules will be realized.

**Acknowledgment.** The authors thank Professor Hayao Kobayashi (Institute for Molecular Science) for helpful discussions. This work was supported by a Grant-in Aid for Scientific Research on Priority Areas (No. 1014901 “Metal-assembled Complexes”) from the Ministry of Education, Science, Sports, and Culture, Japan).

**Supporting Information Available:** Supplementary structure data of [Ni(ptdt)<sub>2</sub>] at 296 and 90 K and atomic coordinates and thermal parameters (PDF). This material is available free of charge via the Internet at <http://pubs.acs.org>. This section tagged

JA9921017

(26) Kato, R.; Kobayashi, H.; Kobayashi, A.; Sasaki, Y. *Chem. Lett.* **1985**, 131–134.